First-Principles Fermi Acceleration in Magnetized Turbulence

Martin Lemoine [*]

Institut d'Astrophysique de Paris, CNRS—Sorbonne Université, 98 bis boulevard Arago, F-75014 Paris, France

This Letter provides a concrete implementation of Fermi's model of particle acceleration in magneto-hydrodynamic (MHD) turbulence, connecting the rate of energization to the gradients of the velocity of magnetic field lines, which it characterizes within a multifractal picture of turbulence intermittency. It then derives a transport equation in momentum space for the distribution function. This description is shown to be substantiated by a large-scale numerical simulation of strong MHD turbulence. The present general framework can be used to model particle acceleration in a variety of environments.

Introduction.—Particle energization through scatterings off inhomogeneous, random moving structures is a universal process [1,2], which has stirred considerable interest in various branches of physics: primarily astrophysics, with applications ranging from solar flares [3] to more remote phenomena involving plasmas in extreme conditions, e.g., [4], but also statistical plasma physics [5] or high-energy density physics [6]. Remarkably, the two papers of Fermi [1,2] represent the first concrete scenarios for the origin of nonthermal particles in the Universe. While the literature has placed significant emphasis on acceleration at shock fronts, numerical experiments have demonstrated that stochastic acceleration can be efficient [7–9], notably so at large turbulent Alfvén velocity [10–14], in the sense that it produces extended, hard power-law distributions of suprathermal particles. Additionally, the stochastic Fermi process assuredly plays a role in the vicinity of shock fronts [15–17], just as it seemingly controls part of the energization in reconnection environments [18,19].

While the overall scenario is commonly pictured as originally formulated by Fermi—a sequence of discrete, pointlike interactions between a particle and infinitely massive, perfectly conducting plasma clouds—its implementation in a realistic turbulent context has remained a challenge [20–22], to the extent that phenomenological applications rely on a Fokker-Planck model parameterized by a momentum diffusion coefficient.

The present Letter proposes a novel approach to this problem and formulates a transport equation to describe the evolution of the distribution function in momentum space. It is first shown that particle momenta obey a continuous-time random walk (CTRW), whose random force scales as the gradients of the velocity of magnetic field lines, coarse grained on a scale comparable to the particle gyroradius $r_g \equiv pc/eB$ (p momentum, $B = |\boldsymbol{B}|$ with $\boldsymbol{B}$ as the magnetic field). A key observation is that those gradients are subject to intermittency on small length scales. Hence, the random forces are neither Gaussian nor white noise in time

and, consequently, the random walk deviates from Brownian motion, just as the transport equation, which is derived here from known properties of CTRW, differs from the Fokker-Planck form. This equation is characterized by the statistics of velocity gradients, which are captured via a multifractal description of turbulence intermittency. This framework is eventually shown to reproduce the time- and momentum-dependent Green's functions obtained by tracking a large number of test particles in a large-scale magnetohydrodynamics (MHD) simulation. The present formalism thus provides a successful implementation of stochastic Fermi acceleration in realistic, collisionless MHD turbulence.

A (continuous-time) random walk picture.—To evaluate energy gains and losses in the original Fermi model, it proves convenient to boost to the scattering center frame where the motional electric field $\boldsymbol{E}$ vanishes. The generalization of that model to a continuous random flow similarly tracks the particle momentum in the instantaneous (here, noninertial) frame $\mathcal{R}_{\not{E}}$ in which $\boldsymbol{E}$ vanishes [23,24], which, in ideal MHD, moves at velocity $\boldsymbol{v_E} = c\boldsymbol{E} \times \boldsymbol{B}/B^2$. In that frame, momentum gains or losses scale in direct proportion to the (lab frame) spatiotemporal gradients of the velocity field $\boldsymbol{v_E}$, as expressed by Γ_{acc}, $\Gamma_{\|}$, and $\Gamma_{\perp}$ below. In detail, the momentum p of particles with gyroradius $r_g \ll \ell_c$ (ℓ_c coherence length of the turbulence) evolves as

$$\dot{p} = p\{\Gamma_{\mathrm{acc}} + \Gamma_{\|} + \Gamma_{\perp}\}, \qquad (1)$$

with $\Gamma_{\mathrm{acc}} = -v^{-1}\mu\boldsymbol{b} \cdot \partial_t\boldsymbol{v_E}$ (where v is the particle velocity; $\mu = \boldsymbol{p} \cdot \boldsymbol{b}/p$ is the pitch-angle cosine with respect to the magnetic field direction $\boldsymbol{b} = \boldsymbol{B}/B$); $\Gamma_{\|} = -\mu^2\boldsymbol{b} \cdot (\boldsymbol{b} \cdot \boldsymbol{\nabla})\boldsymbol{v_E}$ and $\Gamma_{\perp} = -(1-\mu^2)[\boldsymbol{\nabla} \cdot \boldsymbol{v_E} - \boldsymbol{b} \cdot (\boldsymbol{b} \cdot \boldsymbol{\nabla})\boldsymbol{v_E}]/2$. For simplicity, the present Letter focuses on the subrelativistic limit $v_E \ll c$. Equation (1)—more precisely, its relativistic limit—has been shown to account for the bulk of acceleration in

numerical simulations of collisionless turbulence [25], putting the present model on solid footing. It generalizes the two contributions originally identified by Fermi: interactions with moving magnetic mirrors are captured by $\Gamma_\perp$, while orbits in dynamic, curved magnetic field lines are represented by $\Gamma_\parallel$; the remaining term $\Gamma_{\rm acc}$ describes the effective gravity force associated with the acceleration or deceleration of the field lines; of second order in v_E/c, it is subdominant in the subrelativistic limit, unless $v \ll v_A$.

All quantities in Eq. (1) are understood to be coarse grained on wave number scale $k_g \sim r_g^{-1}$ (length scales $l_g \sim 2\pi r_g$), where $r_g = pc/eB$ denotes the particle gyroradius in the lab frame. This procedure filters out wave numbers $k > k_g$, whose contribution averages out over a gyro-orbit, to retain the larger scales that shape the velocity structures responsible for acceleration (in accord with the original Fermi picture).

Henceforth, Eq. (1) is simplified to the symbolic $\dot{p} = p\Gamma_{l_g}$, with Γ_{l_g} representing an aggregate (random) force exerted by electromagnetic fields, coarse grained on scale l_g; order of unity factors related to μ are thus omitted. We also consider relativistic particles ($v \sim c$) to ease the discussion. For technical details concerning the modeling of this random process, see the Supplemental Material, Sec. A [26]. Separate now fluctuations from the mean, $\Gamma_l = \langle\Gamma_l\rangle + \delta\Gamma_l$, the average carrying over the statistical realizations of the turbulent flow: $\langle\Gamma_l\rangle$ characterizes systematic heating, while the random $\delta\Gamma_l$ represents the diffusive part. If $\delta\Gamma_l$ were Gaussian distributed, and its time correlation function that of white noise, the process would describe Brownian motion, in one-to-one correspondence with a Fokker-Planck equation for the distribution function [27]. As anticipated above, however, those random forces are neither Gaussian in amplitude, nor white noise in time: at small scales, they develop large power-law tails as a result of intermittency, while at large scales, the coherence time of the random force $\gtrsim l_g/c$ cannot be regarded as infinitesimal.

To obtain the transport equation, we first observe that the process $\dot{p} = p\Gamma_{l_g}$ can be described as a CTRW: unlike discretized Brownian motion, which operates at a fixed and uniform time step, the random walk is here defined by the joint probability $\phi(p|p';t-t')$ to jump from p' to p in time $\Delta t = t - t'$, with both $\Delta p = p - p'$ and Δt regarded as random variables. Expectations are $\Delta t \sim l_g(p')/c$ (thus, a function of p') and $\Delta \ln p \sim \Gamma_{l_g}\Delta t$. We will assume Δt to be exponentially distributed with mean waiting time $t_p \equiv l_g(p')/c$ and $\Delta \ln p$ distributed as $\Gamma_{l_g}l_g/c$ [$l_g = l_g(p')$]; see the Supplemental Material, Sec. A [26] for methodology. The random walk is then entirely defined by the statistics of the velocity gradients Γ_{l_g}.

Statistics of momentum jumps.—In turbulence theories, such statistics are conveniently described within a multifractal analysis [28–30], which ascribes to each position x a local scaling exponent $h(x)$ for gradients on coarsegraining scale l, viz.

$$\Gamma_l(x) \sim \Gamma_{\ell_c}(x)(l/\ell_c)^{h(x)}, \tag{2}$$

and which describes the set of locations x with index $h(x)$ as a fractal of dimension $d(h)$. The statistics of Γ_l are thus entirely captured by the probability distribution function (PDF) $\mathsf{p}_{\Gamma_{\ell_c}}$ of Γ_{ℓ_c} and by the spectrum $d(h)$, since the probability of being at x in a set with exponent h on scale l evolves as the volume filling fraction $l^{D-d(h)}$ (where D is the number of spatial dimensions). The gradient $\Gamma_{\ell_c}(x)$ on the coherence scale ℓ_c is naturally modeled as a Gaussian variable with standard deviation $\sigma_c \sim v_A/\ell_c$, where v_A denotes the Alfvén velocity of the turbulent component. The spectrum $d(h)$ can take different forms, the simplest being log-normal [31] modern descriptions of the statistics of Elsässer fields in MHD turbulence rather relying on log-Poisson models [32–35]. We use the former log-normal form, as it provides a simple and satisfactory description of the statistics of the gradients of v_E; see the Supplemental Material, Sec. B [26], which includes Refs. [36–39]. We thus derive the PDF p_{Γ_l} of Γ_l as (using $D = 3$) [30]

$$\mathsf{p}_{\Gamma_l} \sim \int d\Gamma_{\ell_c}\mathsf{p}_{\Gamma_{\ell_c}} \int dh\, l^{3-d(h)}\delta[\Gamma_l - \Gamma_{\ell_c}(l/\ell_c)^h]. \tag{3}$$

This PDF remains to be properly normalized. In this formulation, the gradient statistics p_{Γ_l} on all scales reduce to a function of the main quantities v_A, ℓ_c, and the few parameters characterizing $d(h)$, which themselves depend on the physical properties of the turbulence. This offers a first-principles connection between the fundamental statistics of turbulence intermittency and the physics of particle energization.

The transport equation.—The CTRW is exactly equivalent to the following kinetic equation for the volume averaged distribution $n_p(t) = 4\pi p^2 f(p,t)$, where $f(p,t)$ represents the angle-averaged distribution function [40,41],

$$\partial_t n_p(t) = \int_0^{+\infty} dp' \int_0^t dt'[\psi(p|p';t-t')n_{p'}(t')$$
$$- \psi(p'|p;t-t')n_p(t')]. \tag{4}$$

The kernel $\psi(p|p';t-t')$ differs from the CTRW jump distribution probability $\phi(p|p';t-t')$ introduced earlier, yet the two are related as follows. Denoting with a tilde symbol the Laplace transform in time, and ν the Laplace variable conjugate to $t-t'$,

$$\tilde{\psi}(p|p';\nu) = \frac{\nu\tilde{\phi}(p|p';\nu)}{1 - \tilde{\phi}_{p'}(\nu)}, \tag{5}$$

with the shorthand notation $\tilde{\phi}_{p'}(\nu) \equiv \int_0^{+\infty} dp\, \tilde{\phi}(p|p';\nu)$, the subscript p' emphasizing the dependence on p'. As discussed above, we characterize the CTRW with a joint probability distribution of the form

$$\phi(p|p';t-t') = \varphi(p|p')\frac{e^{-(t-t')/t_{p'}}}{t_{p'}}, \qquad (6)$$

recalling that $t_{p'} \equiv l_g(p')/c$. Then,

$$\tilde{\psi}(p|p';\nu) = \frac{\varphi(p|p')}{t_{p'}}, \qquad (7)$$

in which case the transport equation becomes local in time [41],

$$\partial_t n_p(t) = \int_0^{+\infty} dp' \left[\frac{\varphi(p|p')}{t_{p'}} n_{p'}(t) - \frac{\varphi(p'|p)}{t_p} n_p(t) \right]. \qquad (8)$$

It takes the form of a master equation for a Markov process, balancing gains and losses at respective rates $t_{p'}^{-1}$ and t_p^{-1}. As $\varphi(p|p')$ represents the PDF to jump to p from p' in any given amount of time, it is normalized through $\int_0^{+\infty} dp\, \varphi(p|p') = 1$. Recalling that $\Delta \ln p$ is distributed as $\Gamma_{l_g} l_g/c$, the PDF $\varphi(p|p')$ derives from p_{Γ_l} through

$$\varphi(p|p') = \frac{1}{p\, t_{p'}} \mathsf{p}_{\Gamma_{l_g}}, \qquad (9)$$

at $\Gamma_{l_g} = \ln(p/p')/t_{p'}$, with $l_g = l_g(p')$.

Test against numerical experiments.—The above model is now tested on a direct numerical simulation of driven incompressible MHD turbulence (1024^3 with 1024 time steps) [42,43]. This simulation has no guide field, and its units have been set to obtain an Alfvén velocity $v_A = 0.4c$; this offers a reasonable compromise between the limits of applicability of this (subrelativistic) simulation and the value of v_A needed to observe acceleration within the duration of the simulation ($2.8\ell_c/c$); see the Supplemental Material, Sec. B [26] for the methods used to extract numerical data from this simulation.

The statistics of the absolute values of the velocity gradients Γ_l, parallel and perpendicular to the mean magnetic field and coarse grained on scale l, are shown in Fig. 1 for various values of l. The red solid line represents the adjustment obtained for a log-normal spectrum $d(h) = 3 - (h - h_{MF})^2/(2\sigma_{MF}^2)$, parameterized by $h_{MF} = -0.2$ and $\sigma_{MF} = 0.9$, see the Supplemental Material, Sec. B [26]. As the random walk has been simplified to one aggregate force term Γ_l, we have chosen to tune those parameters to provide a fair reconstruction of the ensemble of parallel and perpendicular gradients, rather than fitting one or the other. The solid blue line shows an adjustment of $\mathsf{p}_{|\Gamma_l|}$ by a broken power-law approximation, which has the advantage of speeding up the numerical integration of the kinetic transport equation. It takes the form
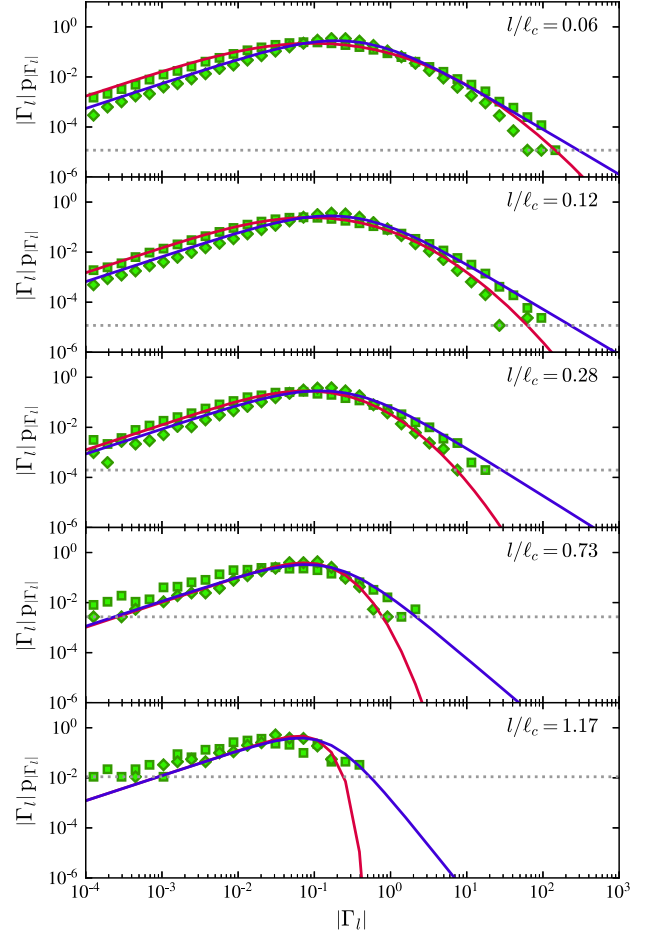

FIG. 1. Statistics $|\Gamma_l|\mathsf{p}_{|\Gamma_l|}$ of the absolute values of the gradients Γ_l (Γ_l expressed in units of c/ℓ_c). Symbols, values recorded in a 1024^3 MHD simulation at various coarse-graining scales l, as indicated; squares (respectively, diamonds), gradients measured along (respectively, perpendicular to) the mean magnetic field direction as coarse grained on scale l. The PDF reveals power-law tails at large values of $|\Gamma_l|$ on small scales. Solid red line, adjustment of a multifractal log-normal model; solid blue line, a broken power-law approximation; dotted line, shot noise level associated with the finite sampling variance.

$$\mathsf{p}_{\Gamma_l} \sim \left[1 + \left(\frac{\Gamma_l}{\sigma_{BP}(l)} \right)^{k_0(l)/k_1} \right]^{-k_1}, \qquad (10)$$

where $\sigma_{BP}(l)$ and $k_0(l)$ depend on l; $\sigma_{BP}(l)$ characterizes the width of the distribution before it turns over into the power-law behavior with index $\simeq -k_0(l)$, while $k_1 = 3$ ensures the smoothness of that transition from core to wing; see the Supplemental Material, Sec. B [26] for details and methodology. Both models use a width $\sigma \simeq 0.3v_A/\ell_c$, with $\sigma = \sigma_c$ for Γ_{ℓ_c} [respectively, $\sigma = \sigma_{BP}(\ell_c)$] for the multi-fractal (respectively, broken power-law) model.

From p_{Γ_l}, we derive $\varphi(p|p')$ using Eq. (9), then integrate the transport equation (8) to compare the theoretical spectra $n_p(t)$ with experimental ones obtained by tracking a large number of particles in the MHD simulation. We remark here
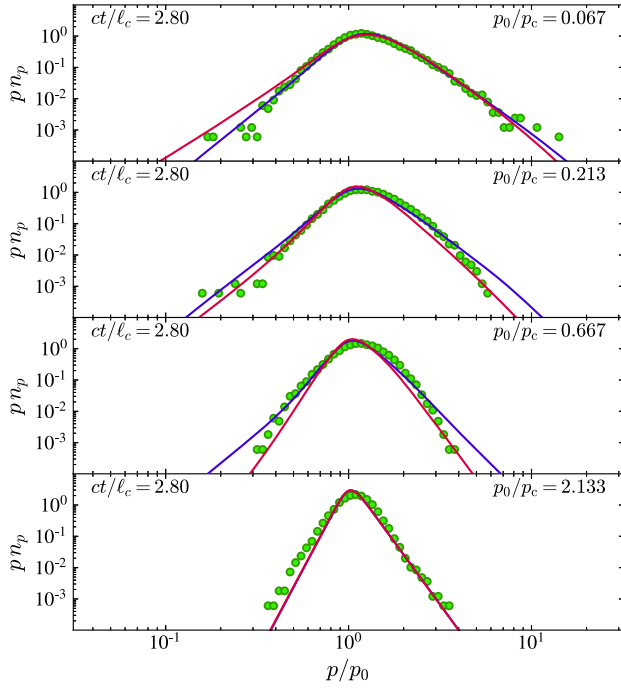
FIG. 2. Particle spectra obtained at the final time $t = 2.8\ell_c/c$ for various initial momenta as indicated in units of p_c; p_c is such that $l_g(p_c) = \ell_c$. The red and blue lines correspond to the two models shown in Fig. 1.
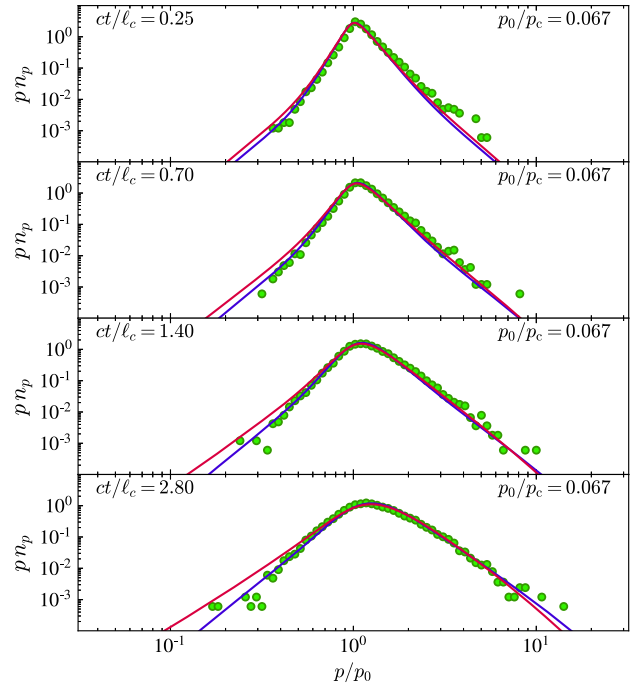
FIG. 3. Same as Fig. 2, now showing the particle spectra at various times, for the smallest initial injection momentum, as indicated.

that, first, those two models for p_{Γ_l} provide slightly different fits to the measured gradient statistics; therefore, the comparison of the corresponding $n_p(t)$ provides a first glance at how the choice of parameters affects those spectra. Second, p_{Γ_l} extends to values of Γ_l beyond the range where it can be measured in the simulation, allowing, in particular, for unbounded gains in momentum over a finite timescale l_g/c; to regularize this, we multiply $\varphi(p|p')$ by a cutoff $\exp[-(\ln p - \ln p')^2]$, which bounds the maximum gain to the order of unity on that timescale. This theoretical maximum is well motivated here, since v_A is not small compared to c [24]; different choices are possible, but the overall influence does not exceed that associated with the uncertainty affecting p_{Γ_l}. Third, the model predicts the evolution of momentum in the frame $\mathcal{R}_{\not\parallel}$; hence the comparison to the experimental $n_p(t)$ requires a boost to the simulation frame, which slightly broadens the particle distribution. To minimize this effect, we inject particles at a given momentum p_0 in the $R_{\not\parallel}$ frame at time $t = 0$, integrate the equation, then boost the theoretical spectrum to the simulation frame. We thus effectively measure a Green's function convoluted with this boost. Finally, the numerical distributions of the velocity gradients have small yet nonzero mean values, implying a slight advection drift toward increasing momenta; it has been taken into account in adjusting p_{Γ_l} to the data. Further details on these procedures are provided in the Supplemental Material, Sec. B [26].

Those theoretical models (red and blue curves, following the conventions of Fig. 1) are compared in Figs. 2 and 3 to the momentum- and time-dependent Green's functions obtained by tracking a large number of test particles in the simulation cube. The test particles have been propagated in the time-dependent snapshots of the simulation; i.e., the time evolution of the electromagnetic fields has been properly taken into account. In Fig. 2, the spectra are plotted vs p/p_0 for increasing values of the initial momentum p_0, from $p_0/p_c = 0.067$ to $p_0/p_c = 2.1$, thus covering a dynamic range of 1.5 decades; p_c denotes the momentum such that $l_g(p_c) = \ell_c$, i.e., the coarse graining becomes comparable to the coherence scale. At $p_0 > p_c$, the spectrum narrows down: the acceleration decreases because the particle then sees the turbulence as a collection of incoherent cells of small extent relative to its gyroradius. In Fig. 3, the spectra are plotted for $p_0/p_c = 0.067$ up to the maximal integration time of the simulation $t = 2.8\ell_c/c$. This rather satisfactory comparison between theoretical and experimental Green's functions supports the present picture.

Discussion and perspectives.—As in the original Fermi picture, the efficiency of acceleration scales with the turbulent Alfvén velocity v_A [44], which controls the magnitude of the random force through its influence on Γ_{ℓ_c}. At lower v_A, one observes a softer spectrum at a given time, but as time passes, the spectrum becomes harder; two different values of v_A eventually give comparable spectra at times rescaled by $1/v_A^2$. Figures 2 and 3

indicate that power-law spectra are generic, as observed in kinetic simulations [10,11]. Those power laws find their origin in the large excursions that particle momenta can undergo in sparse regions of intense gradients [24,45], here captured by the extended wings of $\varphi(p'|p)$. In the absence of those, a Kramers-Moyal expansion would indeed reduce Eq. (8) to the Fokker-Planck form with diffusion coefficient $D_{pp} = \int dp'(p'-p)^2 \varphi(p'|p)/t_p$ and advection coefficient $A_p = \int dp'(p'-p)\varphi(p'|p)/t_p$.

The present scenario naturally accounts for the recent observation that some particles can see their energy increase exponentially fast in localized regions, up to an energy gain of a few [9], by virtue of $\dot{p} = p\Gamma_l$ with Γ_l varying on scales of extent l; see also [24,46]. As scattering is here dominated by magnetic mirrors, which become intermittent on small scales, one also anticipates anomalous spatial transport. Inspection of numerical data confirms that some particles preserve their pitch angles over long distances $\gtrsim \ell_c$, while others suffer strong deflection on short distances. This might account for spatial superdiffusion events observed in recent simulations [47] and trapping in others [8].

The present approach differs from that of Ref. [13], which extracts from numerical experiments empirical momentum-dependent functions $A_p = \langle \Delta p \rangle / \Delta t$ and $D_{pp} = \langle \Delta p^2 \rangle / \Delta t$. It also differs from Ref. [48], which models transport in momentum space through a fractional Fokker-Planck equation, describing the random walk as a Lévy process. The present $\varphi(p'|p)$ is more akin to a truncated Lévy flight, which contains flat tails but well-defined high-order moments. This implies that, at asymptotic times, the random walk will behave as some Brownian motion, due to central-limit convergence; however, the extended wings of $\varphi(p'|p)$ slow down this convergence quite appreciably, as expressed by the Berry-Esséen theorem [49]; hence, for practical matters, the present non-Fokker-Planck form remains required. This transport equation remains amenable to extensions: for instance, wave-particle resonant interactions, if effective [50,51], could be included by adding an extra diffusion term and, similarly, for particle heating in small-scale nonideal electric fields, which ensures injection into the Fermi process in kinetic simulations [10–14]; finally, including standard radiative and escape terms would allow to model the emerging spectra from astrophysical sources.

In summary, the present Letter has established a novel, general framework for implementing stochastic Fermi acceleration in a realistic, collisionless turbulent bath, opening a connection between the statistics of the intermittent gradients of the velocity of magnetic field lines and the rate of energization. Improved insight on turbulence intermittency could ultimately allow a first-principles calculation of particle spectra. The applicability of this formalism thus extends beyond that of the numerical simulation of incompressible MHD turbulence against which it was successfully tested.

---

[*] lemoine@iap.fr

[1] E. Fermi, On the origin of the cosmic radiation, Phys. Rev. **75**, 1169 (1949).

[2] E. Fermi, Galactic magnetic fields and the origin of cosmic radiation, Astrophys. J. **119**, 1 (1954).

[3] V. Petrosian, Stochastic acceleration by turbulence, Space Sci. Rev. **173**, 535 (2012).

[4] A. Tramacere, E. Massaro, and A. M. Taylor, Stochastic acceleration and the evolution of spectral distributions in synchro-self-Compton sources: A self-consistent modeling of blazars' flares, Astrophys. J. **739**, 66 (2011).

[5] G. M. Zaslavskiĭ and B. V. Chirikov, Reviews of topical problems: Stochastic instability of non-linear oscillations, Sov. Phys. Usp. **14**, 549 (1972).

[6] K. A. Beyer, B. Reville, A. F. A. Bott, H.-S. Park, S. Sarkar, and G. Gregori, Analytical estimates of proton acceleration in laser-produced turbulent plasmas, J. Plasma Phys. **84**, 905840608 (2018).

[7] P. Dmitruk, W. H. Matthaeus, N. Seenu, and M. R. Brown, Test particle acceleration in three-dimensional magneto-hydrodynamic turbulence, Astrophys. J. **597**, L81 (2003).

[8] D. Trotta, L. Franci, D. Burgess, and P. Hellinger, Fast acceleration of transrelativistic electrons in astrophysical turbulence, Astrophys. J. **894**, 136 (2020).

[9] O. Pezzi, P. Blasi, and W. H. Matthaeus, Relativistic particle transport and acceleration in structured plasma turbulence, Astrophys. J. **928**, 25 (2022).

[10] V. Zhdankin, G. R. Werner, D. A. Uzdensky, and M. C. Begelman, Kinetic Turbulence in Relativistic Plasma: From Thermal Bath to Nonthermal Continuum, Phys. Rev. Lett. **118**, 055103 (2017).

[11] L. Comisso and L. Sironi, Particle Acceleration in Relativistic Plasma Turbulence, Phys. Rev. Lett. **121**, 255101 (2018).

[12] L. Comisso and L. Sironi, The interplay of magnetically dominated turbulence and magnetic reconnection in producing nonthermal particles, Astrophys. J. **886**, 122 (2019).

[13] K. Wong, V. Zhdankin, D. A. Uzdensky, G. R. Werner, and M. C. Begelman, First-principles demonstration of diffusive-advective particle acceleration in kinetic simulations of relativistic plasma turbulence, Astrophys. J. **893**, L7 (2020).

[14] V. Zhdankin, Particle energization in relativistic plasma turbulence: Solenoidal versus compressive driving, Astrophys. J. **922**, 172 (2021).

[15] Y. Matsumoto, T. Amano, T. N. Kato, and M. Hoshino, Electron Surfing and Drift Accelerations in a

Weibel-Dominated High-Mach-Number Shock, Phys. Rev. Lett. **119,** 105101 (2017).

[16] D. Trotta, F. Valentini, D. Burgess, and S. Servidio, Phase space transport in the interaction between shocks and plasma turbulence, Proc. Natl. Acad. Sci. U.S.A. **118,** e2026764118 (2021).

[17] M. Nakanotani, G. P. Zank, and L. L. Zhao, Turbulence-dominated shock waves: 2D hybrid kinetic simulations, Astrophys. J. **926,** 109 (2022).

[18] J. F. Drake, M. Swisdak, H. Che, and M. A. Shay, Electron acceleration from contracting magnetic islands during reconnection, Nature (London) **443,** 553 (2006).

[19] F. Guo, X. Li, W. Daughton, P. Kilian, H. Li, Y.-H. Liu, W. Yan, and D. Ma, Determining the dominant acceleration mechanism during relativistic magnetic reconnection in large-scale systems, Astrophys. J. **879,** L23 (2019).

[20] A. M. Bykov and I. Toptygin, Particle kinetics in highly turbulent plasmas (renormalization and self-consistent field methods), Phys. Usp. **36,** 1020 (1993).

[21] F. Bouchet, F. Cecconi, and A. Vulpiani, Minimal Stochastic Model for Fermi's Acceleration, Phys. Rev. Lett. **92,** 040601 (2004).

[22] J. W. Burby, A. I. Zhmoginov, and H. Qin, Hamiltonian Mechanics of Stochastic Acceleration, Phys. Rev. Lett. **111,** 195001 (2013).

[23] M. Lemoine, Generalized Fermi acceleration, Phys. Rev. D **99,** 083006 (2019).

[24] M. Lemoine, Particle acceleration in strong MHD turbulence, Phys. Rev. D **104,** 063020 (2021).

[25] V. Bresci, M. Lemoine, L. Gremillet, L. Comisso, L. Sironi, and C. Demidem, Nonresonant particle acceleration in strong turbulence: Comparison to kinetic and MHD simulations, Phys. Rev. D **106,** 023028 (2022).

[26] See Supplemental Material at http://link.aps.org/supplemental/10.1103/PhysRevLett.129.215101 for additional details on the stochastic model (Sec. A) and on the methods used to extract and analyze numerical data from a large-scale simulation of incompressible MHD turbulence (Sec. B).

[27] H. Risken, *The Fokker-Planck Equation. Methods of Solution and Applications* (Springer, Berlin, New York, 1989).

[28] U. Frisch and G. Parisi, On the singularity structure of fully developed turbulence, in *Turbulence and Predictability in Geophysical Fluid Dynamics*, edited by M. Ghil, R. Benzi, and G. Parisi (North Holland, Amsterdam, 1985), pp. 84–87.

[29] R. Benzi, G. Paladin, A. Vulpiani, and G. Parisi, On the multifractal nature of fully developed turbulence and chaotic systems, J. Phys. A **17,** 3521 (1984).

[30] R. Benzi, L. Biferale, G. Paladin, A. Vulpiani, and M. Vergassola, Multifractality in the Statistics of the Velocity Gradients in Turbulence, Phys. Rev. Lett. **67,** 2299 (1991).

[31] B. Dubrulle, Beyond Kolmogorov cascades, J. Fluid Mech. **867,** P1 (2019).

[32] D. Biskamp and W.-C. Müller, Scaling properties of three-dimensional isotropic magnetohydrodynamic turbulence, Phys. Plasmas **7,** 4889 (2000).

[33] W.-C. Müller, D. Biskamp, and R. Grappin, Statistical anisotropy of magnetohydrodynamic turbulence, Phys. Rev. E **67,** 066302 (2003).

[34] P. Padoan, R. Jimenez, Å. Nordlund, and S. Boldyrev, Structure Function Scaling in Compressible Super-Alfvénic MHD Turbulence, Phys. Rev. Lett. **92,** 191102 (2004).

[35] B. D. G. Chandran, A. A. Schekochihin, and A. Mallet, Intermittency and alignment in strong RMHD turbulence, Astrophys. J. **807,** 39 (2015).

[36] Z.-S. She and E. Leveque, Universal Scaling Laws in Fully Developed Turbulence, Phys. Rev. Lett. **72,** 336 (1994).

[37] B. Dubrulle, Intermittency in Fully Developed Turbulence: Log-Poisson Statistics and Generalized Scale Covariance, Phys. Rev. Lett. **73,** 959 (1994).

[38] Y. Yang, M. Wan, W. H. Matthaeus, Y. Shi, T. N. Parashar, Q. Lu, and S. Chen, Role of magnetic field curvature in magnetohydrodynamic turbulence, Phys. Plasmas **26,** 072306 (2019).

[39] K. H. Yuen and A. Lazarian, Curvature of magnetic field lines in compressible magnetized turbulence: Statistics, magnetization predictions, gradient curvature, modes, and self-gravitating media, Astrophys. J. **898,** 66 (2020).

[40] J. Klafter and R. Silbey, Derivation of the Continuous-Time Random-Walk Equation, Phys. Rev. Lett. **44,** 55 (1980).

[41] B. Berkowitz, A. Cortis, M. Dentz, and H. Scher, Modeling non-Fickian transport in geological formations as a continuous time random walk, Rev. Geophys. **44,** RG2003 (2006).

[42] Y. Li, E. Perlman, M. Wan, Y. Yang, C. Meneveau, R. Burns, S. Chen, A. Szalay, and G. Eyink, A public turbulence database cluster and applications to study Lagrangian evolution of velocity increments in turbulence, J. Turbul. **9,** N31 (2008).

[43] G. Eyink, E. Vishniac, C. Lalescu, H. Aluie, K. Kanov, K. Bürger, R. Burns, C. Meneveau, and A. Szalay, Flux-freezing breakdown in high-conductivity magnetohydrodynamic turbulence, Nature (London) **497,** 466 (2013).

[44] In the presence of a mean field B_0 (corresponding Alfvén velocity v_{A0}), $v_A = (\delta B / B_0) v_{A0}$ (δB turbulent component), therefore $\delta B / B_0$ impacts acceleration at fixed v_{A0}.

[45] M. Lemoine and M. A. Malkov, Power-law spectra from stochastic acceleration, Mon. Not. R. Astron. Soc. **499,** 4972 (2020).

[46] G. Brunetti and A. Lazarian, Stochastic reacceleration of relativistic electrons by turbulent reconnection: A mechanism for cluster-scale radio emission?, Mon. Not. R. Astron. Soc. **458,** 2584 (2016).

[47] S. Maiti, K. Makwana, H. Zhang, and H. Yan, Cosmic-ray transport in magnetohydrodynamic turbulence, Astrophys. J. **926,** 94 (2022).

[48] H. Isliker, L. Vlahos, and D. Constantinescu, Fractional Transport in Strongly Turbulent Plasmas, Phys. Rev. Lett. **119,** 045101 (2017).

[49] M. F. Shlesinger, Comment on "Stochastic Process with Ultraslow Convergence to a Gaussian: The Truncated Lévy Flight", Phys. Rev. Lett. **74,** 4959 (1995).

[50] B. D. G. Chandran, Scattering of Energetic Particles by Anisotropic Magnetohydrodynamic Turbulence with a Goldreich-Sridhar Power Spectrum, Phys. Rev. Lett. **85,** 4656 (2000).

[51] H. Yan and A. Lazarian, Scattering of Cosmic Rays by Magnetohydrodynamic Interstellar Turbulence, Phys. Rev. Lett. **89,** 281102 (2002).